Galactic wormholes and black holes.

Chiranjeeb Singha

Inter-University Centre for Astronomy and Astrophysics

July 11, 2024

Reference

- Shauvik Biswas, **Chiranjeeb Singha**, Sumanta Chakraborty, "*Galactic wormholes: Geometry, stability, and echoes,*" **Phys. Rev. D 109, 064043 (2024)**.

- **Chiranjeeb Singha**, Shauvik Biswas, "*Galactic pure Lovelock black holes: Geometry, stability, and Hawking temperature,*" **Phys.Rev.D 109 (2024) 2, 024043**.

Galactic wormholes and black holes

- There are no isolated objects in our universe.

- The flatness of the rotation curves of galaxies, the dynamics of hot gas in clusters, gravitational lensing experiments, among others — 95 percent mass of the galaxy comes from that of non-baryonic matter, namely the dark matter.

- Any compact object, be it a black hole, or, an ECO must reside in an environment involving dark matter.

- The spacetime geometry must be affected by the environment.

Galactic wormholes

- The environmental effects on wormholes residing in a galaxy.

- Two wormhole spacetimes classes: the Damour-Solodukhin wormhole and the braneworld wormhole at the center of galaxies

- How the galactic parameters affect the time domain single, quasinormal modes, photon sphere, innermost stable circular orbits, and shadow radius.

Damour-Solodukhin wormhole

- Damour-Solodukhin wormhole,

$$ds^2 = -\left(1 - \frac{2M_1}{r}\right) dt^2 + \left(1 - \frac{2M_2}{r}\right)^{-1} dr^2 + r^2 d\Omega_2^2 \ ,$$

where $M_2 = M_1(1 + \lambda^2)$.

- The above metric is a solution of Einstein's equations, provided the right-hand side of Einstein's equations involves an energy-momentum tensor with an anisotropic fluid

$$\begin{aligned}
T_\nu^{\mu\,(\mathrm{w})} &= \ \mathrm{diag.} \left(0, p_r^{(\mathrm{ds})}, p_\perp^{(\mathrm{ds})}, p_\perp^{(\mathrm{ds})}\right) \\
p_r^{(\mathrm{ds})} &= \ -\frac{\lambda^2 M_1}{4\pi r^2 (r - 2M_1)} \ , \\
p_\perp^{(\mathrm{ds})} &= \ \frac{(r - M_1)\lambda^2 M_1}{8\pi r^2 (r - 2M_1)^2} \ .
\end{aligned}$$

Damour-Solodukhin wormhole

- The energy density $\rho^{(\mathrm{ds})}$ supporting the wormhole identically vanishes,

- The radial pressure $p_r^{(\mathrm{ds})}$ is non-zero but negative.

- The wormhole spacetime violates both the null and weak energy conditions, as $\rho^{(\mathrm{ds})} + p_r^{(\mathrm{ds})} < 0$, while $\rho^{(\mathrm{ds})} + p_\perp^{(\mathrm{ds})} > 0$.

Geometry of wormholes at the center of galaxies

- We solve the following Einstein's equations,

$$G_{\mu\nu} = T_{\mu\nu}^{(\mathrm{g})} + T_{\mu\nu}^{(\mathrm{w})} \ ,$$

where, $T_{\mu\nu}^{(\mathrm{g})}$ is the energy-momentum tensor for the galactic matter and $T_{\mu\nu}^{(\mathrm{w})}$ is the energy-momentum tensor supporting the wormhole geometry.

- Here,

$$T_{\nu}^{\mu\,(\mathrm{g})} = \mathrm{diag.} \left(-\rho^{(\mathrm{g})}, 0, p_{\perp}^{(\mathrm{g})}, p_{\perp}^{(\mathrm{g})} \right) \ ,$$

where, $\rho^{(\mathrm{g})}$ is the density of the dark matter halo surrounding the central wormhole and $p_{\perp}^{(\mathrm{g})}$ is the transverse pressure.

- The total configuration involving a wormhole and the galactic matter is spherically symmetric and stationary,

$$ds^2 = -f(r)dt^2 + \left(1 - \frac{2m(r)}{r} \right)^{-1} dr^2 + r^2 d\Omega_2^2 \ .$$

- Motivated by the corresponding mass profile for galactic black holes,

$$m(r) = M_2 + \frac{Mr^2}{(r+a)^2} \left(1 - \frac{2M_1}{r}\right) \left(1 - \frac{2M_2}{r}\right) \ .$$

Here, M is the mass, and a is the characteristic radius of the dark matter halo.

- For the above mass function, the g^{rr} component of the metric describing the galactic wormhole becomes,

$$g^{rr} = \left(1 - \frac{2M_2}{r}\right) \left[1 - \frac{Mr}{(r+a)^2} \left(1 - \frac{2M_1}{r}\right)\right] \ .$$

Damour-Solodukhin wormhole at the center of galaxies

- The G_t^t component of the Einstein's equations yield,
  $m'(r) = 4\pi r^2 (\rho_{(ds)}^{(g)} + \rho^{(ds)})$. Since the energy density of matter $\rho^{(ds)}$,
  the following density profile for the galactic dark matter distribution,

$$\rho_{(ds)}^{(g)} = \frac{2M\left(1 - \frac{2M_1}{r}\right)(a + 2M_1)}{4\pi r(a + r)^3} + \lambda^2 \frac{M\left[M_1(r - 4M_1) - aM_1\right]}{2\pi r^2(a + r)^3} \ .$$

Damour-Solodukhin wormhole at the center of galaxies

- The determination of the g_{tt} component of the metric is achieved by solving the G_r^r component of the Einstein's equation,

$$\frac{1}{r}\left(1 - \frac{2m(r)}{r}\right)\frac{d\ln f}{dr} - \frac{1}{r^2} + \frac{1}{r^2}\left(1 - \frac{2m(r)}{r}\right) = 8\pi\left(p_r^{(\mathrm{g})} + p_r^{(\mathrm{ds})}\right) .$$

- For the galactic matter distribution, there is no radial out/inflows present, and hence we must have $p_r^{(\mathrm{g})} = 0$. We find

$$f(r) = \left(1 - \frac{2M_1}{r}\right)e^\gamma , \qquad \gamma \equiv -\pi\sqrt{\frac{M}{\xi}} + 2\sqrt{\frac{M}{\xi}}\tan^{-1}\left(\frac{r + a - M}{\sqrt{M\xi}}\right)$$

where, $\xi \equiv 2a - M + 4M_1$.

Damour-Solodukhin wormhole at the center of galaxies

- The total matter-energy density supporting this wormhole is simply given by $\rho_{(\mathrm{ds})}^{(\mathrm{g})}$, which is positive for $r > 2M_2$, and hence the weak energy condition is satisfied everywhere outside the wormhole.

- The energy density comes from the galactic dark matter, while the radial pressure arises from the matter supporting the wormhole, such that $\rho + p_r \equiv \rho_{(\mathrm{ds})}^{(\mathrm{g})} + p_r^{(\mathrm{ds})}$, among which the contribution by the energy density is positive, while the radial pressure contributes negatively.

- The violation of the null energy condition for the galactic Damour-Solodukhin wormhole happens for a much smaller spatial region ($2M_2 \leq r < r_0$), compared to the Damour-Solodukhin wormhole, where the violation is present throughout the space ($2M_2 \leq r < \infty$).

Damour-Solodukhin wormhole at the center of galaxies

- The radius r_0, below which the violation of the null energy condition happens can be obtained by solving the algebraic equation $\rho + p_r = 0$, which yields,

$$r_0 \simeq 2M_2 + a\sqrt{\frac{M_2}{2M}}\lambda \ ,$$

  definitely greater than the throat location of the wormhole.

- In the presence of a galactic halo, the violation of the null energy condition can be tamed, such that for all space outside the radial coordinate r_0 the null energy condition is satisfied

- One can also show that $\rho + p_\perp$ is positive, as well as $\rho + p_r + 2p_\perp > 0$, for $r \geq 2M_2$. Thus strong energy condition is also satisfied everywhere in the galactic wormhole for $r \geq r_0$.

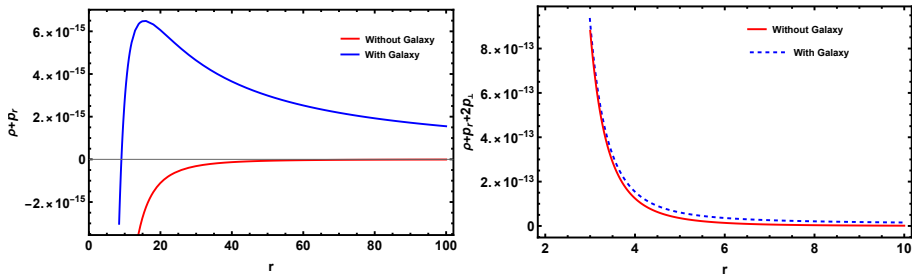# Damour-Solodukhin wormhole at the center of galaxies

Figure: $(a/M_1) = 10^8$, $(M/M_1) = 10^4$, and $\lambda = 10^{-5}$. This plot clearly demonstrates that the null energy condition is violated everywhere in the absence of a dark matter halo. But in the presence of a galaxy, i.e., when the wormhole is surrounded by a dark matter halo, the null energy condition is violated in a small radial interval, close to the throat. On the other hand, the right plane plot presents the variation of $\rho + p_r + 2p_\perp$ with the radial coordinate. As evident, this quantity is indeed positive with or without the galaxy.

The geometry of Damour-Solodukhin wormhole at the center of galaxies.

- $rg'_{tt}(r) = 2g_{tt}$ at $r = r_{\rm ph}$. Solving this algebraic equation the following equation for the photon sphere, to leading order in (M_1/a),

$$r_{\rm ph} = r_{\rm ph} = 3M_1 \left(1 + \frac{MM_1}{a^2} \right) \ .$$

  The presence of a dark matter halo increases the radial location of the photon sphere, compared to the case of an isolated wormhole.

- $V_{\rm eff} = 0$, $V'_{\rm eff} = 0$ and $V''_{\rm eff} = 0$, which provides an algebraic equation for the radial coordinate with the following solution,

$$r_{\rm ISCO} = 6M_1 \left(1 - \frac{32MM_1}{a^2} \right) \ .$$

  The presence of a dark matter halo decreases the radial location of the ISCO, compared to the case of an isolated wormhole.

The geometry of Damour-Solodukhin wormhole at the center of galaxies.

- The calculation of shadow radius involves determining the critical impact parameter associated with null geodesics,

$$r_{\rm sh} = 3\sqrt{3}M_1 \left[1 + \frac{M}{a} + \frac{M(5M - 18M_1)}{6a^2} \right] \ .$$

In the presence of a dark matter halo, the shadow radius will be larger than that of an isolated wormhole.

Ringdown waveform

Comparison of QNM frequencies		
Mode n	For isolated wormhole	For galactic wormhole
1	$0.0321 - 1.083.10^{-4}i$	$0.0326 - 1.2174.10^{-4}i$
2	$0.0638 - 5.720.10^{-4}i$	$0.0649 - 7.6526.10^{-4}i$
3	$0.0950 - 1.679.10^{-3}i$	$0.0967 - 1.9841.10^{-3}i$
4	$0.1258 - 3.709.10^{-3}i$	$0.1280 - 4.0441.10^{-3}i$
5	$0.1566 - 6.739.10^{-3}i$	$0.1592 - 7.0129.10^{-3}i$
6	$0.1877 - 1.0106.10^{-2}i$	$0.1906 - 1.0746.10^{-2}i$
7	$0.2192 - 1.490.10^{-2}i$	$0.2222 - 1.4990.10^{-2}i$
8	$0.2510 - 1.948.10^{-2}i$	$0.2541 - 1.9518.10^{-2}i$
9	$0.2832 - 2.418.10^{-2}i$	$0.2862 - 2.4185.10^{-2}i$
10	$0.3158 - 2.90.10^{-2}i$	$0.3185 - 2.8916.10^{-2}i$

Table: For $l = 0$ and $\lambda = 10^{-5}$. $a = 10^8 M_1$, and $M = 10^4 M_1$. The galactic wormhole is more stable than the isolated one.
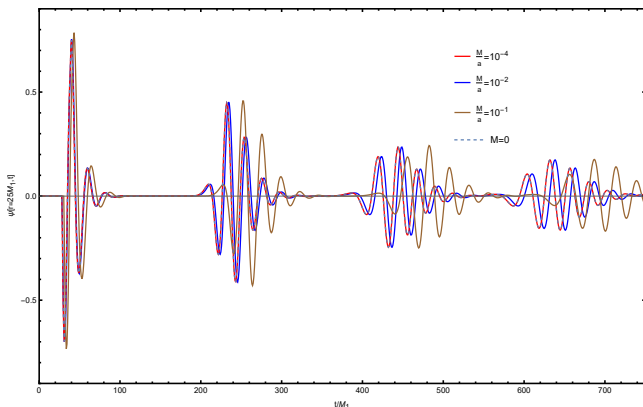
Galactic Damour-Solodukhin wormhole

Figure: This figure is dedicated to a comparison of the ringdown waveform.

Summary

- The presence of the galaxy affects the photon sphere and the shadow radius, causing an increase compared to the isolated counterpart. In contrast, the radial location of the ISCO decreases compared to the isolated counterpart.

- The imaginary parts of the QNM frequencies for the galactic Damour-Solodukhin wormhole are higher compared to the QNM frequencies of the isolated Damour-Solodukhin wormhole, indicating that the presence of galactic matter makes the Damour-Solodukhin wormhole more stable.

- The presence of galactic matter leads to a modification of the potential experienced by the perturbing scalar field, which affects the prompt ringdown.

- This allows us to identify the galactic parameters, independently from the gravitational wave measurements, if echoes are observed in future generations of gravitational wave detectors.

Galactic pure Lovelock black holes

- First-time modeled galactic black holes in pure Lovelock gravity.

- Even though working with higher spacetime dimensions, the Hernquist-type mass profile for the galaxy in such a way that the horizon structure of a pure LoveLock black hole remains intact.

- How the galactic parameters affect the time domain single, quasinormal modes, photon sphere, innermost stable circular orbits, and shadow radius.

- Hawking temperature for the same setup.

The geometry of pure Lovelock black holes in galactic centers.

- The metric for a pure Lovelock black hole of Lovelock order N in d dimensional spacetime,

$$ds^2 = -f(r)dt^2 + f(r)^{-1}dr^2 + r^2 d\Omega_{d-2}^2 .$$

$f(r) = \left(1 - \left(\frac{2^N M_{BH}}{r^{d-2N-1}}\right)^{1/N}\right)$ .The ADM mass is represented as $M_{BH} = (M_{BH}^{1/N})^N$ in this context.

- A modeling approach for the d-dimensional galactic pure Lovelock black hole with a Lovelock order N. The arrangement is expected to remain static, *i.e.*, no radial outflow should be present.

- A perfect fluid with an energy-momentum tensor represented as $T_\nu^\mu = \text{diag.}(-\rho, 0, P_T, P_T)$.

The geometry of pure Lovelock black holes in galactic centers.

- The metric describing the galactic pure Lovelock black hole,

$$ds^2 = -f(r)dt^2 + \left(1 - \left(\frac{2^N m(r)}{r^{d-2N-1}}\right)^{1/N}\right)^{-1} dr^2 + r^2 d\Omega_{d-2}^2 \ .$$

- Here $f(r)$ and $m(r)$ are the two unknown quantities. Motivated by the galactic black hole,

$$
\begin{aligned}
f &= \left(1 - \left(\frac{2^N m(r)}{r^{d-2N-1}}\right)^{1/N}\right) e^\gamma \ , \\
\gamma &= -\pi \sqrt{\frac{M}{\xi}} + 2\sqrt{\frac{M}{\xi}} \tan^{-1} \frac{r + a - M}{\sqrt{M\xi}} \ , \\
\xi &= 2a - M + 4M_{BH} \ .
\end{aligned}
$$

The geometry of pure Lovelock black holes in galactic centers.

- The radial component of the Einstein equation $G^r{}_r = 8\pi T^r{}_r$,

$$\frac{rf'}{2f} = \frac{(d-2N-1)}{N}\frac{(m(r))^{1/N}}{r^{d-2N-1} - 2(m(r))^{1/N}} \ .$$

- Considering terms up to $\mathcal{O}(1/a^2)$, for the $d = 3N + 1$ dimensional galactic pure Lovelock black hole with Lovelock order N as,

$$m(r) = M_{BH} + \frac{NMr^2(M_{BH})^{\frac{N-1}{N}}\left(1 - \frac{2M_{BH}^{1/N}}{r}\right)^2}{a^2} \ .$$

Importantly, this mass distribution ensures the persistence of the horizon of the pure Lovelock black hole.

The geometry of pure Lovelock black holes in galactic centers.

- A ten-dimensional pure Lovelock black hole of Lovelock order three in the galactic center,

$$f = \left(1 - \frac{2M_{BH}^{1/3}}{r}\right) e^{\gamma} .$$

- The mass profile as,

$$m(r) = M_{BH} + \frac{3Mr^2 M_{BH}^{2/3}\left(1 - \frac{2M_{BH}^{1/3}}{r}\right)^2}{a^2} .$$

- Up to $\mathcal{O}(1/a^2)$ and using the mass profile, the g^{rr} component

$$g^{rr} \equiv g(r) = \left(1 - \frac{2M_{BH}^{1/3}}{r}\right)\left(1 - \frac{2Mr\left(1 - \frac{2M_{BH}^{1/3}}{r}\right)}{a^2}\right) .$$

The geometry of pure Lovelock black holes in galactic centers.

- The temporal component of the Einstein equation $G^t{}_t = 8\pi T^t{}_t$,

$$4\pi\rho = \frac{m'(r)}{r^8}$$

$$\Rightarrow \rho = \frac{3MM_{BH}^{2/3}\left(r - 2M_{BH}^{1/3}\right)}{2\pi a^2 r^8} .$$

- Deriving the tangential pressure is facilitated by the Bianchi identities

$$8P_T = \frac{(m(r))^{1/3}\rho}{r - 2(m(r))^{1/3}} .$$

The geometry of pure Lovelock black holes in galactic centers.

- Upto the leading order in $\left(\frac{M_{BH}^{1/3}}{a}\right)$, the radius of the photon sphere is given by,

$$r_{\mathrm{ph}} = 3M_{BH}^{1/3}\left(1 + \frac{MM_{BH}^{1/3}}{a^2}\right) .$$

  The presence of a dark matter halo increases the radial location of the photon sphere, compared to the case of an isolated ten-dimensional pure Lovelock black hole of Lovelock order three.

- The radial coordinate solution of ISCO is given by,

$$r_{\mathrm{ISCO}} = 6M_{BH}^{1/3}\left(1 - \frac{32MM_{BH}^{1/3}}{a^2}\right) .$$

  The presence of a dark matter halo decreases the radial location of the ISCO, compared to the case of an isolated ten-dimensional pure Lovelock black hole of Lovelock order three.

The geometry of pure Lovelock black holes in galactic centers.

- The shadow radius associated with the galactic ten-dimensional pure Lovelock blackhole of Lovelock order three is given by,

$$r_{\rm sh} = 3\sqrt{3}M_{BH}^{1/3}\left[1 + \frac{M}{a} + \frac{M(5M - 18M_{BH}^{1/3})}{6a^2}\right] .$$

In the presence of a dark matter halo, the shadow radius will be larger than that of an isolated ten-dimensional pure Lovelock black hole of Lovelock order three.
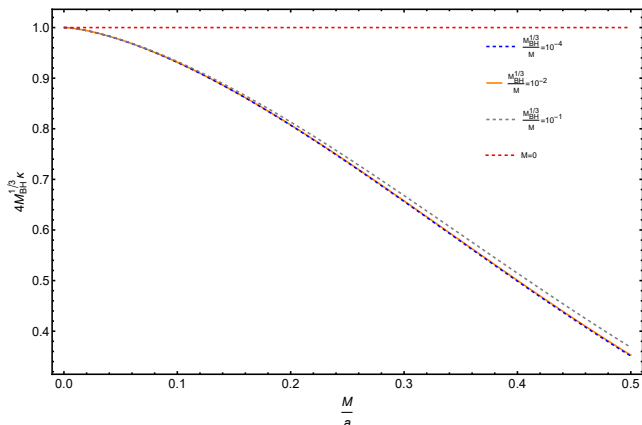
Hawking temperature

Figure: Here we have shown the variation of surface gravity with $\frac{M}{a}$ for various galactic parameters. The introduction of a dark matter halo causes a reduction in the Hawking temperature when compared to the scenario of an isolated ten-dimensional pure Lovelock black hole of Lovelock order three.

Ringdown waveform of galactic pure Lovelock black hole

Comparison of QNM frequencies		
Mode n	For ten-dimensional isolated pure Lovelock black hole of order three	For ten-dimensional galactic pure Lovelock black hole of order three
0	$0.7330 - 0.0912i$	$0.7259 - 0.0894i$
1	$0.7189 - 0.2756i$	$0.7121 - 0.2701i$
2	$0.6917 - 0.4660i$	$0.6859 - 0.4566i$
3	$0.6542 - 0.6662i$	$0.6494 - 0.6521i$
4	$0.6104 - 0.8794i$	$0.6066 - 0.8590i$
5	$0.5673 - 1.1071i$	$0.5614 - 1.0778i$
6	$0.5282 - 1.3446i$	$0.5175 - 1.3075i$
7	$0.5042 - 1.5916i$	$0.4778 - 1.5460i$

Table: For $\ell = 1$ and $\frac{M}{a} = 10^{-2}$. In this case, the values are more or less in agreement, with the isolated pure Lovelock black hole being more stable than the galactic one.
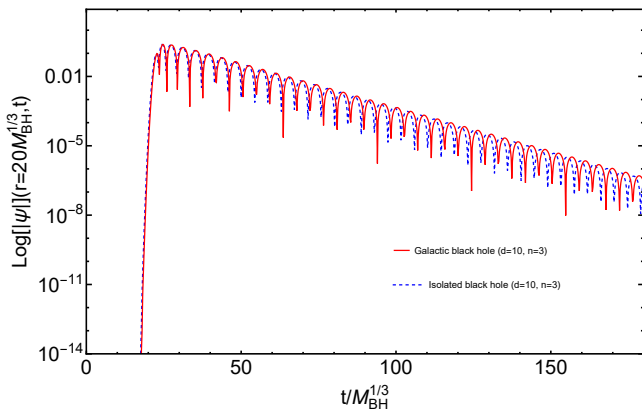
Galactic pure Lovelock black holes

Figure: This figure is dedicated to a comparison of the ringdown waveform of galactic pure Lovelock black holes to its isolated counterpart. Considered $d = 10$ and $N = 3$. r_*^0 lies outside of the corresponding photon sphere. The galactic parameters $\frac{M}{a} = 10^{-2}$.

Summary

- Galactic black holes within the framework of pure Lovelock gravity. The spacetime metric is obtained by considering the Hernquist-type mass profile for the galaxy, resulting in a pure Lovelock black hole situated at the galaxy's center.

- The $d = 3N + 1$ galactic pure Lovelock black hole of Lovelock order N.

- The presence of the galaxy affects the photon sphere and the shadow radius, causing an increase compared to the isolated counterpart. In contrast, the radial location of the ISCO decreases compared to the isolated counterpart.

- The presence of a dark matter halo decreases the Hawking temperature compared to the scenario of an isolated pure Lovelock black hole.

Summary

- The imaginary parts of the QNM frequencies for the galactic pure Lovelock black hole are smaller compared to those of the isolated pure Lovelock black hole, indicating that the presence of a galaxy renders the pure Lovelock black hole less stable.

- The presence of galactic matter leads to a modification of the potential experienced by the perturbing scalar field, which affects the prompt ringdown.

- This information could be valuable in identifying galactic parameters as well as distinguishing them from their isolated pure Lovelock counterparts and the GR counterparts theoretically or in future experimental observations but the effect of extra dimension in pure Lovelock gravity must be reduced to $d = 4$ by some mechanism (e.g., compactification).

Stability of galactic wormholes under scalar perturbation

- The scalar field Ψ can be considered as a test scalar field, living in the background geometry of of the galactic wormholes and satisfying the massless Klein-Gordon equation, $g^{\mu\nu}\nabla_\mu\nabla_\nu\Psi = 0$.

$$\Psi(t, r, \theta, \phi) = \frac{1}{r}\sum_{l=0}^{\infty}\sum_{m=-l}^{l} e^{-i\omega t} Y_{lm}(\theta, \phi)\psi_{lm}(r) \ .$$

Here, $Y_{lm}(\Omega)$ corresponds to the spherical harmonics, and $\psi_{lm}(r)$ is the radial function that needs to be determined.

- The radial part of the scalar field,

$$\frac{d^2\psi_{lm}}{dr_*^2} + \left[\omega^2 - V_l(r)\right]\psi_{lm} = 0 \ .$$

Stability of galactic wormholes under scalar perturbation

- The tortoise coordinate r_*

$$\frac{dr_*}{dr} = \frac{1}{\sqrt{g^{rr}g_{tt}}} = \sqrt{\frac{r}{f(r)\left[r - 2m(r)\right]}} \ .$$

- The potential $V_l(r)$ is given by,

$$V_l(r) = f(r)\frac{l(l+1)}{r^2} + \frac{\sqrt{f(r)\left[1 - 2m(r)/r\right]}}{r}\partial_r\left(\sqrt{f(r)\left[1 - 2m(r)/r\right]}\right)$$

- Explicit expressions for the mass function and the function $f(r)$.

The geometry of GR black holes

- The metric for the Schwarzshild black hole

$$ds^2 = -f(r)dt^2 + f(r)^{-1}dr^2 + r^2 d\Omega^2 \ ,$$

  $f(r) = (1 - 2M_{BH}/r)$. M_{BH} is the mass of the black hole.

- The algebraic equation $rf' = 2f$ enabling the determination of the photon sphere's radius (r_{ph}). For the Schwarzschild spacetime

$$r_{\mathrm{ph}} = 3M_{BH} \ .$$

The geometry of GR black holes

- A motion of a massive particle in spacetime and impose the following three conditions: $V_{\mathrm{eff}} = 0$, $V'_{\mathrm{eff}} = 0$, and $V''_{\mathrm{eff}} = 0$. For the Schwarzschild spacetime,

$$r_{\mathrm{ISCO}} = 6M_{\mathrm{BH}} \ .$$

- The calculation of r_{sh} involves determining the critical impact parameter associated with null geodesics. For Schwarzschild spacetime leads to,

$$r_{sh} = 3\sqrt{3}M_{BH} \ .$$

The geometry of GR black holes in galactic centers

- For a GR black hole in the galactic center, a perfect fluid of energy-momentum tensor $T_\nu^\mu = \text{diag.}(-\rho, 0, P_T, P_T)$.

- The spherical symmetric metric for this system in the following manner [1],

$$ds^2 = -f(r)dt^2 + \left(1 - \frac{2m(r)}{r}\right)^{-1} dr^2 + r^2 d\Omega^2 \ .$$

- The mass profile as $m(r) = M_{BH} + \frac{Mr^2}{(r+a)^2}\left(1 - 2M_{BH}/r\right)^2$.

- M is the total mass of the "halo" and a is a typical length scale associated with the dark matter distribution in the galaxy.

- This mass profile maintains the structure of the GR black hole horizon.

---

[1] V. Cardoso, K. Destounis, F. Duque, R. P. Macedo, and A. Maselli, "Black holes in galaxies: Environmental impact on gravitational-wave generation and propagation," Phys. Rev. D 105 no. 6, (2022) L061501.

The geometry of GR black holes in galactic centers

- The radial component of Einstein equation $G^r{}_r = 8\pi T^r{}_r$,

$$\frac{rf'}{2f} = \frac{m(r)}{r - 2m(r)} \ .$$

- The solution of the above equation,

$$
\begin{aligned}
f &= \left(1 - \frac{2M_{BH}}{r}\right) e^{\gamma} \ , \\
\gamma &= -\pi\sqrt{\frac{M}{\xi}} + 2\sqrt{\frac{M}{\xi}} \tan^{-1}\frac{r + a - M}{\sqrt{M\xi}} \ , \\
\xi &= 2a - M + 4M_{BH} \ .
\end{aligned}
$$

The geometry of GR black holes in galactic centers

- The temporal component of the Einstein equation, given by $G^t{}_t = 8\pi T^t{}_t$,

$$
\begin{aligned}
4\pi\rho &= \frac{m'(r)}{r} \\
\Rightarrow \rho &= \frac{2M(a + 2M_{BH})(1 - 2M_{BH}/r)}{4\pi r(a + r)^3} .
\end{aligned}
$$

- The tangential pressure can be obtained from the Bianchi identities,

$$
2P_T = \frac{m(r)\rho}{r - 2m(r)} .
$$

The geometry of GR black holes in galactic centers

- Upto the leading order in $\left(\frac{M_{BH}}{a}\right)$, the radius of the photon sphere,

$$r_{\rm ph} = 3M_{BH}\left(1 + \frac{MM_{BH}}{a^2}\right) .$$

  The presence of a dark matter halo increases the radial location of the photon sphere, compared to the case of an isolated Schwarzschild black hole.

- The radial coordinate solution of ISCO,

$$r_{\rm ISCO} = 6M_{BH}\left(1 - \frac{32MM_{BH}}{a^2}\right) .$$

  Introducing a dark matter halo reduces the radial location of the ISCO position relative to the isolated Schwarzschild black hole scenario.

The geometry of GR black holes in galactic centers

- The shadow radius associated with the galactic blackhole,

$$r_{\rm sh} = 3\sqrt{3}M_{BH}\left[1 + \frac{M}{a} + \frac{M(5M - 18M_{BH})}{6a^2}\right] \, .$$

In the presence of a dark matter halo, the shadow radius will be larger than that of an isolated Schwarzschild black hole.

Hawking temperature

- For $d = 10$ and $N = 3$ dimensional galactic pure Lovelock blackhole.

$$\kappa = e^{\frac{3}{2}\beta} \frac{\sqrt{1 + \frac{4MM_{BH}^{1/3}}{a^2}}}{4M_{BH}^{1/3}} \ .$$

- β as a shorthand for the quantity,

$$\beta = \sqrt{\frac{M}{2a - M}} \left[2\tan^{-1} \left(\frac{a - M}{\sqrt{M(2a - M)}} \right) - \pi \right] \ .$$

- The Hawking temperature is defined as $T_H = \kappa/2\pi$.

Stability of galactic pure Lovelock black holes under scalar perturbation

- The scalar field Ψ can be considered as a test scalar field, living in the background geometry of the galactic pure Lovelock blackhole and satisfying the massless Klein-Gordon equation, $g^{\mu\nu}\nabla_\mu\nabla_\nu\Psi = 0$.

$$\Psi(t, r, \Omega) = \frac{1}{r^{(d-2)/2}} \sum_{l=0}^{\infty} \sum_{m=-l}^{l} e^{-i\omega t} Y_{lm}(\Omega)\psi_{lm}(r) .$$

Here, $Y_{lm}(\Omega)$ corresponds to the spherical harmonics, and $\psi_{lm}(r)$ is the radial function that needs to be determined.

- The radial part of the scalar field,

$$\frac{d^2\psi_{lm}}{dr_*^2} + \left[\omega^2 - V_l(r)\right]\psi_{lm} = 0 .$$

Stability of galactic pure Lovelock black holes

- The tortoise coordinate r_*

$$\frac{dr_*}{dr} = \frac{1}{\sqrt{g^{rr}g_{tt}}} = \sqrt{\frac{1}{f(r)g(r)}} \ .$$

- The potential $V_l(r)$ is given by,

$$
\begin{aligned}
V_l(r) &= f(r)\left[\frac{l(l+d-3)}{r^2} + \frac{(d-2)(d-4)}{4r^2}g(r)\right.\\
&+ \left.\frac{(d-2)}{4r}\left(g'(r) + \frac{f'(r)}{f(r)}g(r)\right)\right] \ .
\end{aligned}
$$

- Explicit expressions for the mass function and the function $f(r)$.